Electronic Structure of La0.5Ca0.5MnO3

Boer, P.K. de; Leuken, H. van; Groot, R.A. de; Rojo, T.; Barberis, G.E.

Published in:
Solid State Communications

DOI:
10.1016/S0038-1098(97)00055-0

Publication date:
1997

Pergamon

Solid State Communications, Vol. 102, No. 8, pp. 621–626, 1997

0038–1098/97 $17.00+.00

PII: S0038–1098(97)00055-0

ELECTRONIC STRUCTURE OF $La_{0.5}Ca_{0.5}MnO_3$

P.K. de Boer,[a] H. van Leuken,[a] R.A. de Groot,[a] T. Rojo[b,*] and G.E. Barberis[b]

[a]Toernoooiveld 1, 6525 ED, Nijmegen, The Netherlands
[b]Instituto de Física, UNICAMP CP 6165, 13083-970 Campinas (SP) Brasil

(*Received* 6 *November* 1996; *accepted* 8 *January* 1997 *by C.E.T. Gonçalves da Silva*)

Electronic structure calculations on $La_{0.5}Ca_{0.5}MnO_3$ are reported. Calculations were performed with the Full Potential LAPW method within the Local Density Approximation (LDA) as well as the Generalised Gradient Approximation (GGA). The ferromagnetic phase of $La_{0.5}Ca_{0.5}MnO_3$ is half-metallic, which is important in the relation to the colossal magnetoresistance properties of this compound. © 1997 Elsevier Science Ltd

Keywords: A. metals, A. magnetically ordered materials, D. electronic structure.

There has recently been much interest in the magnetism and the transport properties of $La_{1-x}Ca_xMnO_3$ and related manganites [1, 2]. The manganites with $0.2 < x < 0.5$ are ferromagnetic and their resistivity depends strongly on the temperature. An external magnetic field can lower the resistivity by several orders of magnitude, resulting in colossal magnetoresistance (CMR). Both the resistivity and the CMR peak at or near the Curie temperature.

$La_{0.5}Ca_{0.5}MnO_3$ lies on the cross-over between ferromagnetic ($x < 0.5$) and antiferromagnetic ($x > 0.5$) behaviour [3]. We calculated the electronic structure of this system for ferromagnetic as well as A-type antiferromagnetic arrangement of the Mn ions. The crystal structure of the ferromagnetic phase is cubic according to several authors [4–6]. Also an orthorhombic structure is reported [7], but no details about the sample preparation and possible deviations from perfect stoichiometry are given. We assume a cubic crystal with a lattice constant $a = 7.2411$ atomic units.

The substitution of La by Ca was performed by taking two cubes of the perovskite $LaMnO_3$ above each other and replacing one La atom by a Ca atom, resulting in a tetragonal unit cell with $c = 2a$. The Full Potential LAPW method [8] was used, i.e. no shape approximations to the potential were assumed. The standard set of basis functions was supplemented with local orbitals for better description of semicore states and to avoid numerical errors due to the linearisation process. Approximately 1500 LAPW's were used. The Brillouin zone integration was performed on a special mesh of 75 k-points. The Generalised Gradient Approximation (GGA), in the parametrisation by Perdew *et al.* [9], is used but a comparison with LDA-calculations is made to indicate the small difference between GGA and LDA in this system. The atomic radii are 2.0 atomic units for the La and Ca atoms and 1.8 atomic units for the Mn and O atoms.

Figure 1 shows the GGA total density of states of the ferromagnetic phase of $La_{0.5}Ca_{0.5}MnO_3$ for both spin directions. This figure shows that $La_{0.5}Ca_{0.5}MnO_3$ is half-metallic: metallic for majority spin electrons, but semiconducting with a gap of 1.5 eV for minority spin electrons. The magnetic moment per unit cell is therefore necessarily integer. In this case it is 7 μ_B, or 3.5 μ_B per Mn atom. There are not many reports on saturated magnetic moments in $La_{0.5}Ca_{0.5}MnO_3$. A moment of 2.2 μ_B is reported in $La_{0.52}Ca_{0.48}MnO_3$ at low temperatures [3], but the moment was not fully saturated. If $A^{3+}_{1-x}B^{2+}_xMnO_3$ is half-metallic, the saturated magnetic moment at zero temperature should be $4-x$ per Mn atom. Some reports indicate such a moment [10, 11], others give some deviations of tenths of μ_B [12, 13] or more. However, oxygen defects often play a substantial role and the moments are not always fully saturated.

The bands between 7.5 eV and 1.5 eV below the Fermi energy have primarily O 2*p* character. Around

*Permanent address: Departamento de Química Inorgánica, Universidad del País Vasco, Spain.

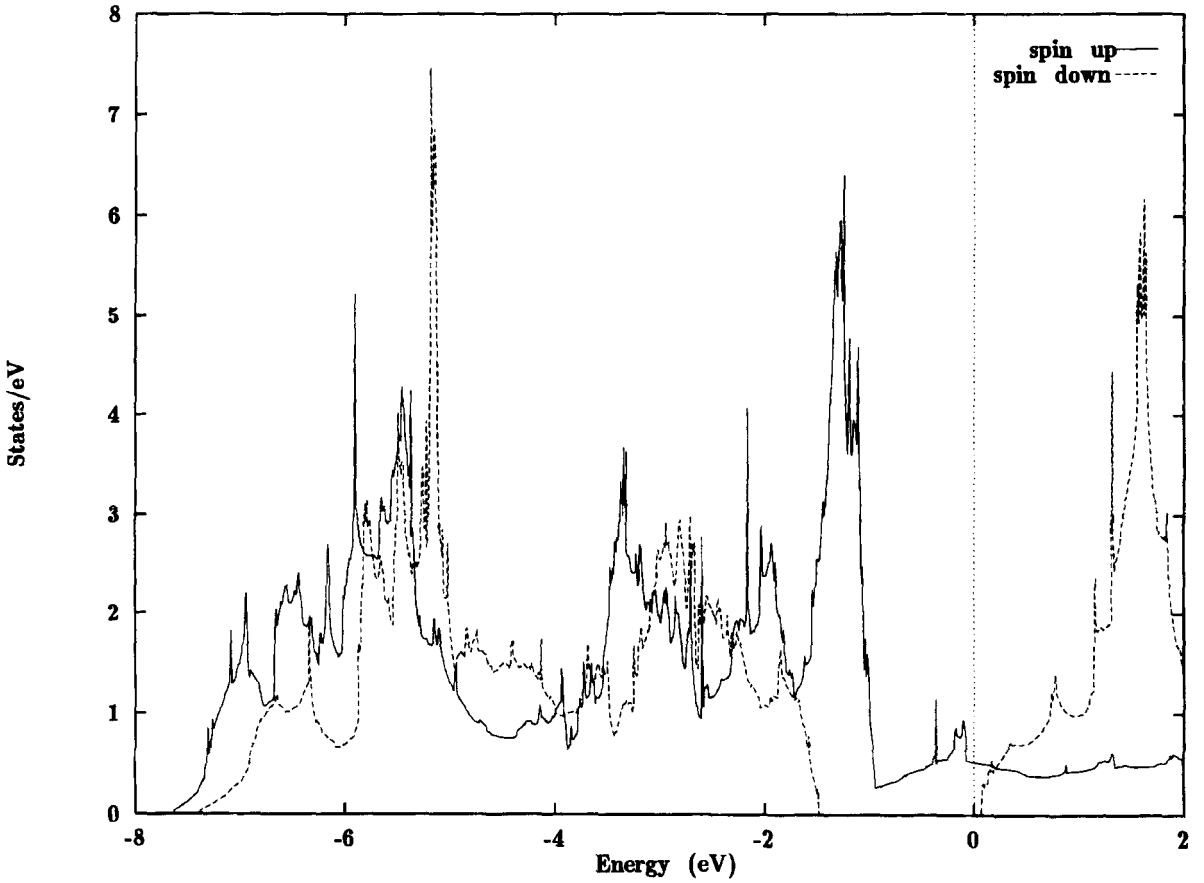

Fig. 1. Total DOS of ferromagnetic $La_{0.5}Ca_{0.5}MnO_3$, calculated within GGA.

1 eV below the Fermi energy lie the spin up Mn t_{2g} bands. The Fermi energy crosses a broad band of Mn e_g orbitals strongly mixed with O 2*p* orbitals, which is in agreement with spectroscopy experiments [14, 15]. The density of states at the Fermi energy is low. The wave functions at the Fermi energy have 69% Mn 3*d* character and 23% O 2*p* character. Thus the band structure confirms the widespread assumption of localised t_{2g} electrons and non-localised e_g electrons. This can also be seen in the magnetic moment. The moment within a Mn sphere, is 2.94 μ_B. The remaining part of the moment is spread out over the oxygen atoms (0.07 μ_B per O atom) and the interstitial space. At 3 eV above the Fermi energy lie the La 4*f* states (not shown in the DOS figure). There is a small difference between GGA and LDA in this system. The LDA [16] total density of states is shown in Fig. 2. For the spin up direction almost no difference between the GGA and the LDA results can be seen. The conduction band of the spin down direction, with primarily Mn t_{2g} character, has decreased in energy a little bit, as compared to the GGA band structure. This has two consequences. First, the gap between the valence band and the conduction band has decreased to 1.4 eV. Second, the Fermi energy lies in the conduction band. Therefore the LDA results show metallic character instead of half-metallic. The nearly half-metallic character of the LDA results has also been reported by others [17]. The electronic structure of transition-metal oxides is an area where there liability of LDA is not always assured. However, enough experience exists to know what the consequences of a better treatment than LDA, be it self-interaction correction or LDA + U etc., will be. Both corrections lead to increased band gaps because of the lowering in energy of occupied states and/or the increase in energy of empty states. It is thus expected that, if a further improvement beyond GGA will influence the band structure, the distance between the Fermi energy and the conduction band of the non-conducting spin direction will increase.

The magnetic structure of $La_{0.5}Ca_{0.5}MnO_3$ depends on the temperature. Below a temperature T_N (150–180 K) it is antiferromagnetically ordered but for $T_N < T < T_C$ (220–230 K) ferromagnetic [3, 7]. The crystal structure of AFM $La_{0.5}Ca_{0.5}MnO_3$ is not clear. Radaelli *et al.* reported an orthorhombic structure [7], as well as for the FM phase, but with different lattice parameters.

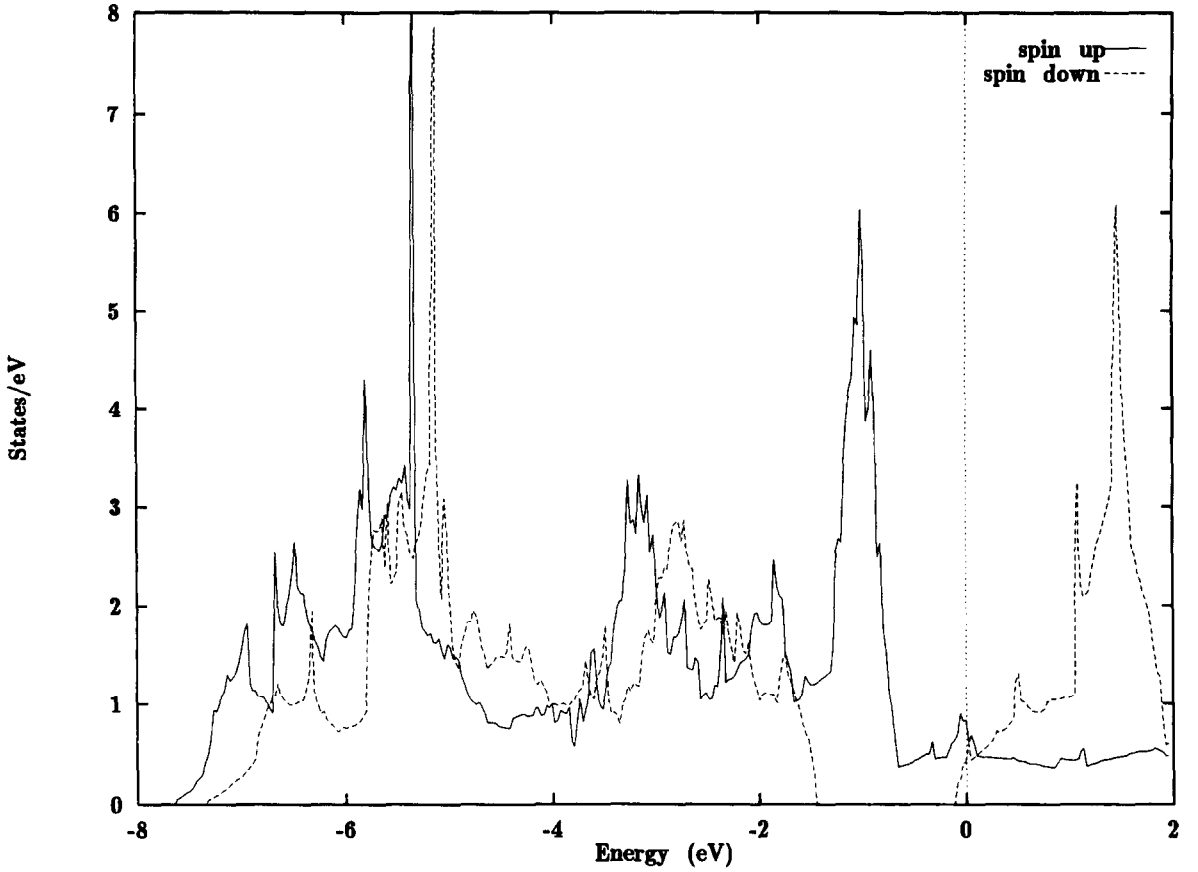

Fig. 2. Total DOS of ferromagnetic $La_{0.5}Ca_{0.5}MnO_3$, calculated within LDA.

More reports of a structural transition, accompanying a FM to AFM transition, in $A^{3+}_{1-x}B^{2+}_{x}MnO_3$ have been published [13, 18, 19]. According to Gong *et al.* the crystal structure of $La_{1-x}Ca_xMnO_3$ stays cubic when x passes 0.5 [4]. Earlier a tetragonal structure for $x > 0.5$ is reported [20]. We calculated, within GGA, A-type AFM $La_{0.5}Ca_{0.5}MnO_3$ in the same structure as in the calculations for the ferromagnetic phase.

The total energy of the AFM phase is 9 meV lower than the FM total energy. This confirms the fact that the ground state at zero temperature is antiferromagnetic. The total DOS of the AFM phase is shown in Fig. 3. In this structure AFM $La_{0.5}Ca_{0.5}MnO_3$ is metallic. In the orthorhombic phase, AFM $La_{0.5}Ca_{0.5}MnO_3$ has a very high resistivity at low temperatures [7] so the structure is presumably very important for the transport properties. Further calculations should be performed for other crystal structures.

The relation between magnetic and transport properties in manganites has been dedicated to the double exchange mechanism [21]. In this theory electronic transport is performed by hopping of electrons from one Mn ion to the other. The Mn ions are assumed to be atomic-like and to follow the Hund rules. Therefore an electron on a Mn^{3+} $(t^3_{2g}e_g)$ ion can only hop to a neighbouring Mn^{4+} (t^3_{2g}) ion if these two ions are parallel aligned. The hopping must occur via oxygen atoms, which lie between the Mn atoms in the perovskite structure. An electron hops from a Mn atom to an oxygen atom and simultaneously another electron, with the same spin, hops from the oxygen atom to the next Mn atom. So according to this double exchange mechanism conduction is only possible through aligned Mn atoms.

However, the e_g conduction electrons are not localised at the Mn atoms, but are bandlike because of their substantial oxygen character. It is therefore essential to treat these electrons in a band picture. As we have shown, the band structure confirms the assumption that conduction is only possible if the Mn atoms are parallel aligned. In fact, the double exchange mechanism can be viewed as the atomic limit of the half-metallic band picture.

We now address the relation between the half-metallic properties and the occurrence of CMR. At zero temperature the magnetisation points uniformly in one direction. The majority spin electrons can travel easily through this domain. At non-zero temperature small domains with magnetisations in other directions are formed. They increase in size and number if the

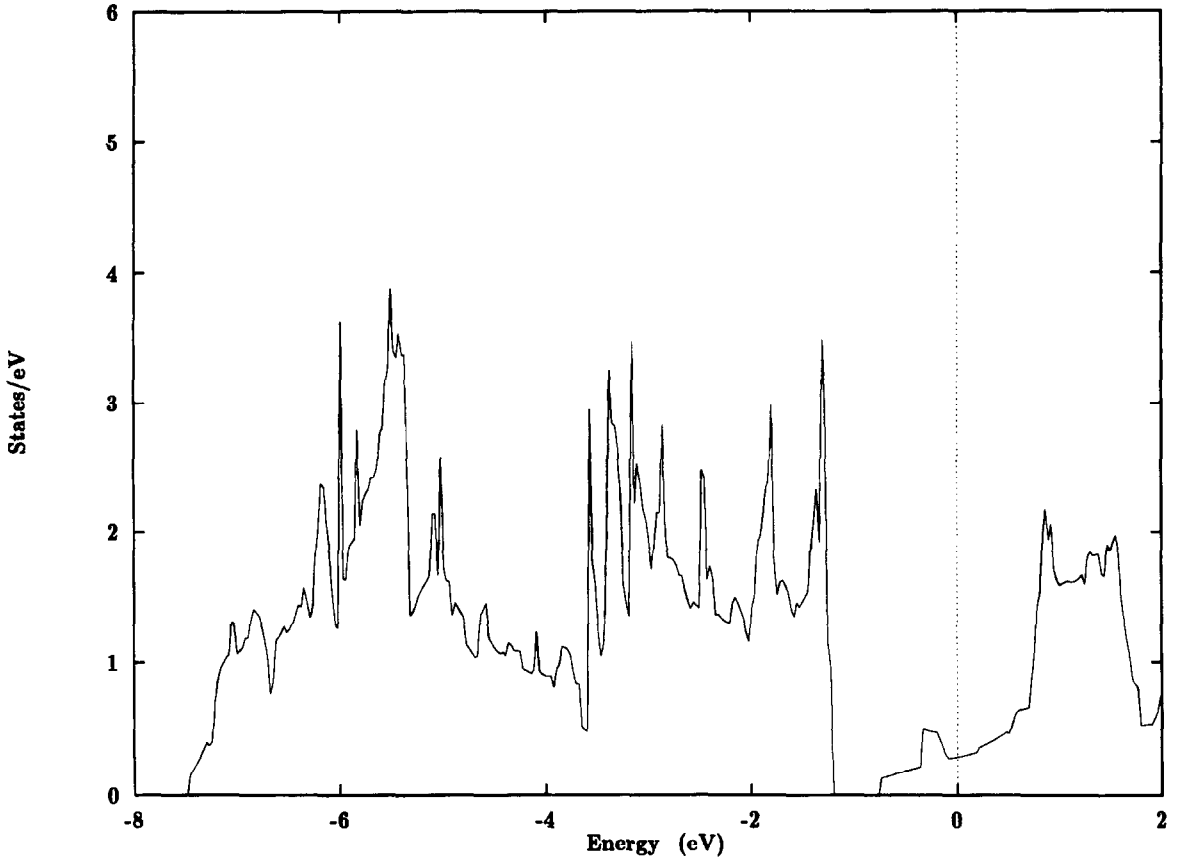

Fig. 3. Total DOS of A-type antiferromagnetic $La_{0.5}Ca_{0.5}MnO_3$.

temperature increases. Assuming that the half-metallic properties within these domains are preserved, walls between regions of opposite magnetisation are insulating. When the temperature reaches the Curie temperature, the correlation length diverges. Thus reaching the Curie temperature there are less and less percolating paths for the majority spin electrons and therefore the resistivity increases. When a magnetic field is switched on, the domains are aligned, resulting in a low resistivity and a large magnetoresistance. The effect of this mechanism is enhanced if the dimensionality of the system is decreased, because of the reduced degree of freedom to create percolating paths. Experiments show indeed that thin films exhibit larger values of CMR than bulk samples. And also in the layered perovskite $(La,Sr)_{n+1}Mn_nO_{III n+1}$, in which conduction primarily occurs within the pseudo-two dimensional Mn–O planes, the highest CMR values are found for the lowest n [22]. Recently this behaviour of the resistivity in half-metallic ferromagnetic manganites has been described, below and above the Curie temperature, by an Ising-like model [23].

Considering the origin of the half-metallic magnetism, it should be stressed that this is quite different from the half-metallic magnetism in the Heusler C_{1b} alloys, where it was first discovered [24]. In the latter case it proved to be quite subtle, the Heusler C_{1b} structure being pseudo-isostructural and the minority spin direction (the non-metallic one) being iso-electronic with the well known III–V semiconductors. The origin of the half-metallic behaviour here is much simpler. Strong magnets are defined by the fact that the d-shell for one spin direction is either completely filled or empty, e.g. nickel. That nickel is not half-metallic originates from the non-polarised s-band. In compound formation these itinerant electrons are transferred to the anions. Hence the manganites are strongly magnetic ionic compounds and all strongly magnetic ionic compounds should be half-metallic. In this sense there is a close resemblance with CrO_2 [25]. The delicate crystal structure and composition dependence of the half-metallic properties, as found in the Heusler alloys, is not to be expected here.

Finally we address the question why the perovskites show unusual magnetoresistances while they have not been reported for half-metallic ferromagnets like the Heusler alloys [26–28]. There are two aspects on the perovskites which are distinct from the Heusler alloys. First of all, the charge carriers in the Heusler alloys are

free electron like with effective masses at about unity, while the charge carriers in the perovskites are bandlike for the e_g, but much more localised. As a consequence, the thickness of the interface between volumes of opposite magnetisation (defined as the distance between the positions of the occurrence of genuine half-metallic behaviour in the two volumes) is one atomic distance for the perovskites [29], but is probably substantially larger for the Heusler alloys. The second difference is the spin-flip probability. The charge carriers in the Heusler alloys have primarily Sb character ($l = 1$) which shows a large spin–orbit interaction. The states in the perovskites which possibly can contribute to the spin–flip probability are the La $4f$ states, but they are located quite far above the Fermi energy (in practice even more than the LDA calculations show). Experiments to test the validity of the half-metallic properties of the manganites are highly desirable. An indirect test is provided by accurate determination of the magnetic moment and the actual composition of $La_{1-x}Ca_xMnO_{3-y}$. The half-metallic properties predict a moment of $4 - x + 2y$. In the archetype of half-metallic magnets, NiMnSb, a crucial experiment proved to be spin–resolved positron annihilation [30, 31]. Such experiments are highly desirable on $La_{1-x}Ca_xMnO_3$ as well. Since CMR is so closely related to half-metallic behaviour in our model it is also desirable to perform magnetoresistance measurements on CrO_2.

In conclusion, we presented GGA and LDA calculations on $La_{0.5}Ca_{0.5}MnO_3$ for the FM and A-type AFM phase in a cubic crystal structure. The AFM phase is lowest in energy, in agreement with experiment. The FM phase is half-metallic, which can be important with respect to the CMR in manganites.

Acknowledgements—This project is supported by the Technology Foundation (STW) and is also part of the research programme of the Stichting voor Fundamenteel Onderzoek der Materie (FOM) and was made possible by financial support from the Nederlandse Organisatie voor Wetenschappelijk Onderzoek (Dutch Organization for Scientific Research, NWO). We acknowledge financial support from Fapesp, Brazil. Discussions with H.J.F. Knops and P.J.M. Bastiaansen are acknowledged.

REFERENCES

1. Kusters, R.M., Singleton, J., Keen, D.A., McGreevy, R. and Hayes, W., *Physica*, **B155,** 1989, 362.
2. von Helmolt, R., Wecker, J., Holzapfel, B., Schultz, L. and Samwer, K., *Phys. Rev. Lett.*, **71,** 1993, 2331.
3. Schiffer, P., Ramirez, A.P., Bao, W. and Cheong, S.-W., *Phys. Rev. Lett.*, **75,** 1995, 3336.
4. Gong, G.-Q., Canedy, C., Xiao, G., Sun, J.Z., Gupta, A. and Gallagher, W.J., *Appl. Phys. Lett.*, **67,** 1995, 1783.
5. Mahesh, R., Mahendiran, R., Raychaudhuri, A.K. and Rao, C.N.R., *J. Solid State Chem.*, **114,** 1995, 297.
6. Mahendiran, R., Tiwary, S.K., Raychaudhuri, A.K., Ramakrishnan, T.V., Mahesh, R., Rangavittal, N. and Rao, C.N.R., *Phys. Rev.*, **B53,** 1996, 3348.
7. Radaelli, P.G., Cox, D.E., Marezio, M., Cheong, S.W., Schiffer, P.E. and Ramírez, A.P., *Phys. Rev. Lett.*, **75,** 1995, 4488.
8. Blaha, P., Schwarz, K., Dufek, P. and Augustyn, R., WIEN95, Technical University of Vienna 1995. (Improved and updated Unix version of the original copy-righted WIEN-code, which was published by Blaha, P., Schwarz, K., Sorantin, P. and Trickey, S.B., *Comput. Phys. Commun.*, **59,** 1990, 399).
9. Perdew, J.P., Chevary, J.A., Vosko, S.H., Jackson, K.A., Pederson, M.R., Singh, D.J. and Fiolhais, C., *Phys. Rev.*, **B46,** 1992, 6671.
10. Jia, Y.X., Lu, L., Khazeni, K., Crespi, V.H., Zettl, A. and Cohen, M.L., *Phys. Rev.*, **B52,** 1995, 9147.
11. Liu, J.Z., Chang, I.C., Irons, S., Klavins, P., Shelton, R.N., Song, K. and Wasserman, S.R., *Appl. Phys. Lett.*, **66,** 1995, 3218.
12. Hwang, H.Y., Cheong, S.-W., Radaelli, P.G., Marezio, M. and Batlogg, B., *Phys. Rev. Lett.*, **75,** 1995, 914.
13. Urushibara, A., Moritomo, Y., Arima, T., Asamitsu, A., Kido, G. and Tokura, Y., *Phys. Rev.*, **B51,** 1995, 14103.
14. Saitoh, T., Bocquet, A.E., Mizokawa, T., Namatame, H., Fujimori, A., Abbate, M., Takeda, Y. and Takano, M., *Phys. Rev.*, **B51,** 1995, 13942.
15. Zhang, J., McIlroy, D.N., Dowben, P.A., Liou, S.H., Sabirianov, R.F. and Jaswal, S.S., *Solid State Commun.*, **97,** 1996, 39.
16. Perdew, J.P. and Wang, Y., *Phys. Rev.*, **B45,** 1992, 13244.
17. Pickett, W.E. and Singh, D.J., *Phys. Rev.*, **B53,** 1996, 1146.
18. Lees, M.R., Barrat, J., Balakrishnan, G., Paul, D. McK. and Yethiraj, M., *Phys. Rev.*, **B52,** 1995, 14303.
19. Asamitsu, A., Moritomo, Y., Tomioka, Y., Arima, T. and Tokura, Y., *Nature*, **373,** 1995, 407.
20. Wollan, E.O. and Koehler, W.C., *Phys. Rev.*, **100,** 1955, 545.
21. de-Gennes, P.-G., *Phys. Rev.*, **118,** 1960, 141.
22. Moritomo, Y., Asamitsu, A., Kuwahara, H. and Tokura, Y., *Nature*, **380,** 1996, 141.
23. Bastiaansen, P.J.M. and Knops, H.J.F. (unpublished).
24. de Groot, R.A., Mueller, F.M., van Engen, P.G. and Buschow, K.H.J., *Phys. Rev. Lett.*, **50,** 1983, 2024.
25. Schwarz, K., *J. Phys.*, **F16,** 1986, L211.
26. Otto, M.J., van Woerden, R.A.M., van der Valk, P.J., Wijngaard, J., van Bruggen, C.F., Haas, C. and Buschow, K.H.J., *J. Phys.: Cond. Matt.*, **1,** 1989, 2341.
27. Otto, M.J., van Woerden, R.A.M., van der Valk, P.J., Wijngaard, J., van Bruggen, C.F. and Haas, C., *J. Phys.: Cond. Matt.*, **1,** 1989, 2351.

28. Otto, M.J., private communication.
29. These conclusions were derived from supercell calculations and will be reported later.
30. Hanssen, K.E.H.M., Mijnarends, P.E., Rabou, L.P.L.M. and Buschow, K.H.J., *Phys. Rev.*, **B42,** 1990, 1533.
31. Surikov, V.V. and Stetsenko, P.N., *Izvestiya AkademiiNauk Seriya Fizicheskaya*, **58,** 1994, 44.